What excited tsunami from Tonga 2022 eruption? Observation and theory

Yasuhiro Nishikawa (nishikawa.yasuhiro@kochi-tech.ac.jp)
Kochi University of Technology https://orcid.org/0000-0003-2084-1440
Masa-Yuki Yamamoto
Kochi University of Technology
Kensuke Nakajima
Kyushu University
Islam Hamama
Kochi University of Technology https://orcid.org/0000-0001-9296-412X
Hiroaki Saito
Hokkaido University https://orcid.org/0000-0001-7937-2971
Yoshihiro Kakinami
Hokkaido Information University

Article

Keywords:

Posted Date: April 13th, 2022

DOI: https://doi.org/10.21203/rs.3.rs-1513574/v1

Abstract

Tsunamis are commonly generated by earthquakes beneath the ocean floor, volcanic eruptions, and landslides. The mysterious tsunami following the Tonga eruption of 2022 is believed to be excited by the atmospheric pressure fluctuations generated by the explosion of this volcano. However, it is not clarified observationally and theoretically that which atmospheric fluctuations excited the tsunami. We show the atmospheric waves that possibly excited the tsunami based on observations detected by our own-manufactured sensors in Japan. The atmospheric fluctuations are classified into Lamb waves, acoustic waves, and gravity waves. The arrival time of the gravity wave and atmosphere-ocean coupling simulation show that the gravity wave propagated at a phase speed of 200-220 m/s, coinciding with tsunami velocity in the Pacific Ocean and suggesting that the gravity wave resonantly excited the tsunami (Proudman resonance). These observations and theory provide an essential basis for theoretical investigations of volcano-induced meteo-tsunamis, including the Tonga event.

Introduction

At 4:10 (UTC) January 15, 2022, the volcano Hunga Tonga-Hunga Ha'apai in Tonga erupted, completely destroying the volcanic island. The eruption scale of VEI (Volcanic Explosivity Index) 6 is said to be a "once in a century" occurrence. Japan Meteorological Agency (JMA) released information at 10:00 (UTC) concerning the possibility of a volcanic induced sea-level variation whose amplitude should be smaller than the advisory level. However, at approximately 11:00 (UTC), 7 hours after the eruption, significant sea-level change began on the coastlines of Japan, amplifying to 0.9 m and 1.2 m at least two local ports (Kuji N36.5 E140.6 and Amami N28.3 E129.4) around 15:00 UTC, after which JMA issued Tsunami Warning. This sequence of events was surprising and anxious both because the observed arrival time of the tsunami was about 2 hours earlier than the conventionally estimated time of 9 hours obtained for the tsunamis excited at the volcano and propagated with usual velocity in the sea and because it grew exceeding the initially estimated amplitude. Hereafter, based on observation and numerical modelling, we will consider the whole event from the explosive eruption to the development of the observed tsunami by coupling atmospheric- and oceanic- waves. The impulsive shock wave, directly resulting from the volcanic eruption, turned into long-period atmospheric waves. Their pressure fluctuations were observed worldwide as a spreading ripple. Some of the long-period atmospheric waves can propagate long distances with little attenuation trapped within the lower ~100km of the atmosphere.

These long-period waves reached Japan, travelling approximately 8,000 km away from the volcano over the Pacific Ocean. Twenty-five comprehensive infrasound sensors (SAYA INF01) installed along the Pacific coastline of Japan by Kochi University of Technology (KUT)[1] detected long-period pressure waves (Fig. 1). Here, we refer to infrasound as a low-frequency sound wave below 20 Hz, the lower limit of audible sound, propagating at the speed of sound through the atmosphere as pressure changes. Infrasound and atmospheric gravity waves are generated by a wide range of geophysical events, such as volcanic eruptions[2,3], thunders, tsunamis[4,5], landslides, meteoroid impacts[6,7], and artificial sources including rocket launches, chemical explosions[8]. The dense KUT infrasound sensor network mainly

installed along the Pacific side of Japan has been operated since 2016 for detecting tsunami-induced acoustic/gravity waves and studying their application for future disaster mitigation.

KUT comprehensive sensors can detect infrasound and gravity wave signals with periods between approximately 0.2 and 500 s that conventional barometers are hard to observe. The sensor also has a barometer, a three-component accelerometer, a thermometer, and a differential pressure gauge primary infrasound sensor (microbarometer) at each infrasound observation site. Combining these measurements at the same site helps understand the nature of waves. Fig. 1 includes a quick look at the infrasound and barometer signals observed at three sites of the KUT sensor network. Usually, a signal is extracted by the correlation analysis among simultaneous observations because waveforms at remote stations are contaminated by local noise. However, in the case of the current Tonga volcanic eruption, the similarities among the waveforms observed by the 25 KUT stations across all of Japan are evident without the correlation analysis, indicating an intense coherent signal, namely, the vastness of the Tonga eruption event. The pressure variation, which continued for several hours in Japan, is not generated by a single wave but by multiple wave packets traveling multiple paths at different speeds constrained by the dispersion relation[9,10] of waves under the effects of gravity and temperature inhomogeneity in the atmosphere. For example, low-frequency signals can propagate horizontally as gravity waves but cannot propagate vertically if the frequency is below the acoustic cut-off (approximately 3.2 mHz at 15 °C, ground pressure condition); only high-frequency sound waves can propagate vertically. As a result of the propagation properties, even if the sound emitted from the same source propagates at the speed of sound, the path and arrival time differ depending on their frequencies.

In this paper, we will perform frequency analysis on the observed infrasound/gravity wave datasets to identify both the long-period Lamb waves and gravity waves and the short-period acoustic waves with different propagating paths to show the characteristics of each type of wave, mainly in terms of velocity/celerity difference and path. Further, we will also discuss a numerical simulation conducted to understand the eruption of Tonga and the atmosphere-induced meteorological tsunami.

Observations

The pressure waves of the Tonga volcanic eruption reached Japan, 8,000 km away, approximately 7 hours after the eruption. Its speed was estimated as 310 m/s, which is interpreted as the average speed of sound for the lower atmosphere (Fig. 2). The pressure variation continued for several hours. The frequency analyses of pressure waves concerning the arrival time of each wave packet showed that it contained four-wave categories: one long period Lamb wave, two short period acoustic waves, and one long period gravity wave (Fig. 3), which have different wave celerity, a kind of apparent speed as a function of distance from the sound source to the sensor.

The earliest arriving component seen in Fig. 3 is the Lamb wave[11]. This pressure wave is trapped at approximately 20 km altitude from the ground surface and propagates at the sound speed averaged over the wave trapping region. The component has a wide frequency range that was extended below the

detection limit of the infrasound sensors. The datasets of barometers showed that the peak pressure change was approximately 200 Pa, and the period of passing the half-wavelength was approximately 1000 s. It is known that such low-frequency Lamb waves barely attenuate and can easily travel a path of several thousand kilometers. Even the Lamb wave signals that propagate from the other side of the Earth, or those that encircle the Earth more than once, are later observed. The observed presence of the Lamb wave component strongly implies that the eruption mainly generated Lamb waves with periods as long as or even longer than 200 seconds, suggesting the vast magnitude of the explosion event.

The second and third arrivals seen in Fig. 3 are acoustic waves in 0.003–0.05 Hz. These waves arrived approximately 2,000 and 10,000 seconds after the first Lamb wave arrival. These acoustic waves are higher in frequency than the Lamb waves. They can propagate with a vertical velocity component under the vertical profile of sound speed, which depends on the air temperature at each local region along the path. Each second and third wave has a wave celerity of 290 and 230 m/s, respectively, calculated from the horizontal distances from the sound source to the sensor and arrival times of observations. If the wave originated from the same sound source, the third wave would have an exceptionally high attenuation in the high-frequency band above 1 Hz.

The fourth arrival seen in Fig. 3 is the gravity wave. Steady oscillations of approximately 10 minutes were observed following the sound waves at many sites (Fig. 1). The lower curve in Fig. 3b, the lowermost-frequency component of the differential pressure gauge, clearly shows the arrival of the gravity wave. According to the accompanying barometers, raw amplitudes of the oscillations exceed 20 Pa at many stations. Although the waveform of the changes slightly differs from station to station, the observation time began earlier in the south and later in the north, which is consistent with the idea that a wave packet propagated as a kind of internal gravity wave at approximately 200–220 m/s from the Tonga volcano.

Gravity waves excited Tsunami over the Pacific Ocean.

The gravity wave observed by KUT sensors could be the origin of the tsunami generated by the Tonga volcanic eruption through Proudman resonance[12]. It should be emphasized that this propagation speed is close to the typical tsunami speed in the Pacific Ocean. Both gravity and tsunami waves presumably travelled with almost the same speed of 200–220 m/s (Fig. 4). Moreover, the reported time (11:00 UTC) of sea-level fluctuations along the Japanese coastline was well correlated to the arrivals of the wave packet of the gravity wave. To understand the possible behaviour of gravity waves and tsunamis in the interaction process, we implemented illustrative two-dimensional numerical modelling based on the hydrodynamic equations describing the dynamic coupling of a compressible atmosphere with oceanic tsunamis below it (see Methods 2). The result shows that the explosive release of heat in the stratosphere excites all candidates of observed waves, i.e., Lamb waves that are trapped near the ground surface, acoustic gravity waves that propagate with “bouncing” between the ground and mesopause (~ 90 km), and gravity waves that have a vertically modal structure between the ground surface and mesopause and dispersedly propagate with a wide range of horizontal speeds, including those of tsunamis. Some acoustic waves bear large amplitudes into the thermosphere and possibly disturb the ionosphere[13].

Tsunamis are indeed excited resonantly by the gravity waves, despite that the amplitude of the corresponding gravity waves is much smaller than that of Lamb or acoustic waves. Notably, the gravity wave-tsunami resonance occurs over a relatively wide range of characteristic velocities. Close examination reveals that tsunamis are excited by gravity waves whose phase speed is comparable to tsunamis (~ 200 m/s). These waves propagate collectively as a “wave packet” with a group velocity that is slower than the phase speed of the tsunami. It is also notable in the time evolution (Supplementary Movie). The tsunamis amplify gradually within a region located a few hundred km from the volcano, and the amplitude scarcely changes afterward. This implies that the high tsunamis that struck the islands of Tonga within several kilometers require excitation mechanisms other than the gravity waves, such as pyroclastic flow and submarine landslides, whose effects should be considered elsewhere.

It has been observed that the sea level fluctuation increased along the coast of Japan around the beginning of the detected gravity wave packet.

It also implies that the observed coincidence of the arrivals of gravity waves and tsunamis should be interpreted not as the continuous resonance between the gravity waves and tsunamis but as their propagations in tandem after resonant amplification in the region relatively close to the volcano. This point remains verified by careful comparison between barometric and tsunami observations over the Pacific.

Two packets of acoustic wave

We have identified two kinds of ray paths for acoustic waves. One is refracted from the stratosphere; the other is refracted from the lower thermosphere. According to the three-dimensional ray-tracing calculations of infrasound emitted by a volcano eruption[10], the celerity of some of the waves turning from the stratosphere is approximately 300 m/s, and those from the lower thermosphere are approximately 238 m/s. The parabolic equation method[14] was applied to estimate the two-dimensional transmission loss of acoustic energy in the azimuth direction toward Japan (see Methods 1). Moreover, the sound waves turning from the lower thermosphere have a lower frequency than those from the stratosphere. These numerical results are consistent with the observation (Fig. 3b). In this calculation, the third wave is coming through the lower thermospheric path for the longer propagating distance. In these calculations, several bounces on the sea surface are needed to reach Japan, suggesting that the acoustic waves travelled back and forth between the atmosphere and the ocean surface multiple times.

What Tonga atmospheric waves taught us

We identified the wave propagation characteristics that are excited by global-scale volcanic eruptions. Four-wave packets are observed to be almost similar/coherent among the 25 sites in Japan categorized into Lamb waves, two paths of acoustic waves, and atmospheric gravity waves. Lamb wave and our simple equation give us the yield and lower estimation of the explosive energy of the Tonga eruption. The total energy is 46 ± 14 megatons (see Methods 3), one of the most significant energy we have ever encountered. Acoustic waves with several bounces on the sea surface are needed to reach Japan,

suggesting that the infrasound travelled back and forth between the atmosphere and the ocean surface multiple times. These significant eruptions have allowed us to see the global vertical energy exchange in the atmosphere. Both waves give us great geoscientific suggestions. Lamb waves and acoustic waves are issues in the geoscience field, but the last gravity wave contains a more prominent theme. The gravity wave excited an unexpected tsunami in the Pacific Ocean. The velocity of the gravity waves strikingly well matched the velocity of tsunamis, resulting in the coupling of the gravity waves with the tsunami and the generation of an unpredictable tsunami. The tsunami was also excited even in the Caribbean Sea, separated by American continent. In other words, this tsunami could occur anywhere on earth. Thus, gravity waves are of interest not only for geoscience but also for disaster mitigation.

Declarations

Data availability

The data that support the findings of this study are openly available in “Kochi University of Technology Infrasound Observation Network System” at http://infrasound.kochi-tech.ac.jp/infrasound/graph.php. The source code of the numerical model used for the atmosphere-tsunami coupling simulation can be obtained from the authors with reasonable requests.

Acknowledgments

This research was made possible through grants from MEXT Grant-in-Aid for Special Purposes Project/Area (No. 21K21353), JSPS KAKENHI (Grant No. JP17H02062), the SECOM Science and Technology Foundation, the Murata Science Foundation (Grant No. M20AN115), NEXCO Group Companies’ Support Fund to Disaster Prevention Measures on Expressways, and Earthquake Res. Inst., the University of Tokyo, Joint Research program (2014-B-15 and 2018-B-04). MYY would like to acknowledge all of their support from these fundings.

Author contributions

Y.N. and M. -Y.Y. conducted this project. Y.N. and I.H. carried out the data collection and analysis. K.N. generated gravity wave simulation and its theory. I.H. and H.S. contributed to simulating parabolic equation and yield estimation. Y.K contributed upper atmospheric modelling. Y.N wrote the manuscript. M.-Y.Y. and Y.K provided the data. All authors discussed the results and reviewed the manuscript.

Competing interests

The authors declare no conflict of interest.

Additional information

Correspondence and requests for materials should be addressed to nishikawa.yasuhiro@kochi-tech.ac.jp.

References

1. Yamamoto, M.-Y. & Yokota, A. Infrasound monitoring for disaster prevention from geophysical destructions. in *Proceedings of the 5th International Symposium on Frontier Technology* 24–28 (Kunming, China, 2015).
2. Mikumo, T. & Bolt, B. A. Excitation mechanism of atmospheric pressure waves from the 1980 Mount St Helens eruption. Geophys. J. Int. **81**, 445–461 (1985).
3. Harkrider, D. & Press, F. The Krakatoa air-sea waves: an example of pulse propagation in coupled systems. Geophys. J. Int. **13**, 149–159 (1967).
4. Mikumo, T. et al. Low-frequency acoustic-gravity waves from coseismic vertical deformation associated with the 2004 Sumatra-Andaman earthquake (Mw = 9.2). J. Geophys. Res. **113**, B12402 (2008).
5. Watada, S. Radiation of acoustic and gravity waves and propagation of boundary waves in the stratified fluid from a time-varying bottom boundary. J. Fluid Mech. **627**, 361–377 (2009).
6. Whipple, F. J. W. The great Siberian meteor and the waves, seismic and aerial, which is produced. Q. J. R. Meteorol. Soc. **56**, 287–304 (1930).
7. Brown, P. G. et al. A 500-kiloton airburst over Chelyabinsk and an enhanced hazard from small impactors. Nature **503**, 238–241 (2013).
8. Hamama, I. et al. Investigation of near-surface chemical explosions effects using seismo-acoustic and synthetic aperture radar analyses. J. Acoust. Soc. Am. **151**, 1575–1592 (2022).
9. Watada, S. & Kanamori, H. Acoustic resonant oscillations between the atmosphere and the solid earth during the 1991 Mt. Pinatubo eruption. J. Geophys. Res. **115**, B12319 (2010).
10. Saito, H., Yamamoto, T., Nakajima, K., Kuramoto, K. & Yamamoto, M. y. Identification of the infrasound signals emitted by explosive eruption of Mt. Shinmoedake by three-dimensional ray tracing. *J. Acoust. Soc. Am.* **149**, 591–598 (2021).
11. Garces, M. A., Hansen, R. A. & Lindquist, K. G. Traveltimes for infrasonic waves propagating in a stratified atmosphere. Geophys. J. Int. **135**, 255–263 (1998).
12. Proudman, J. The effects on the sea of changes in atmospheric pressure. Geophys. J. Int. **2**, 197–209 (1929).
13. Kamogawa, M. et al. A possible space-based tsunami early warning system using observations of the tsunami ionospheric hole. *Scientific reports* **6**.**1** (2016): 1–7.
14. Waxler, R. M., Assink, J. D., Hetzer, C. & Velea, D. NCPAprop—a software package for infrasound propagation modeling. J. Acoust. Soc. Am. **141**, 3627–3627 (2017).

Figures

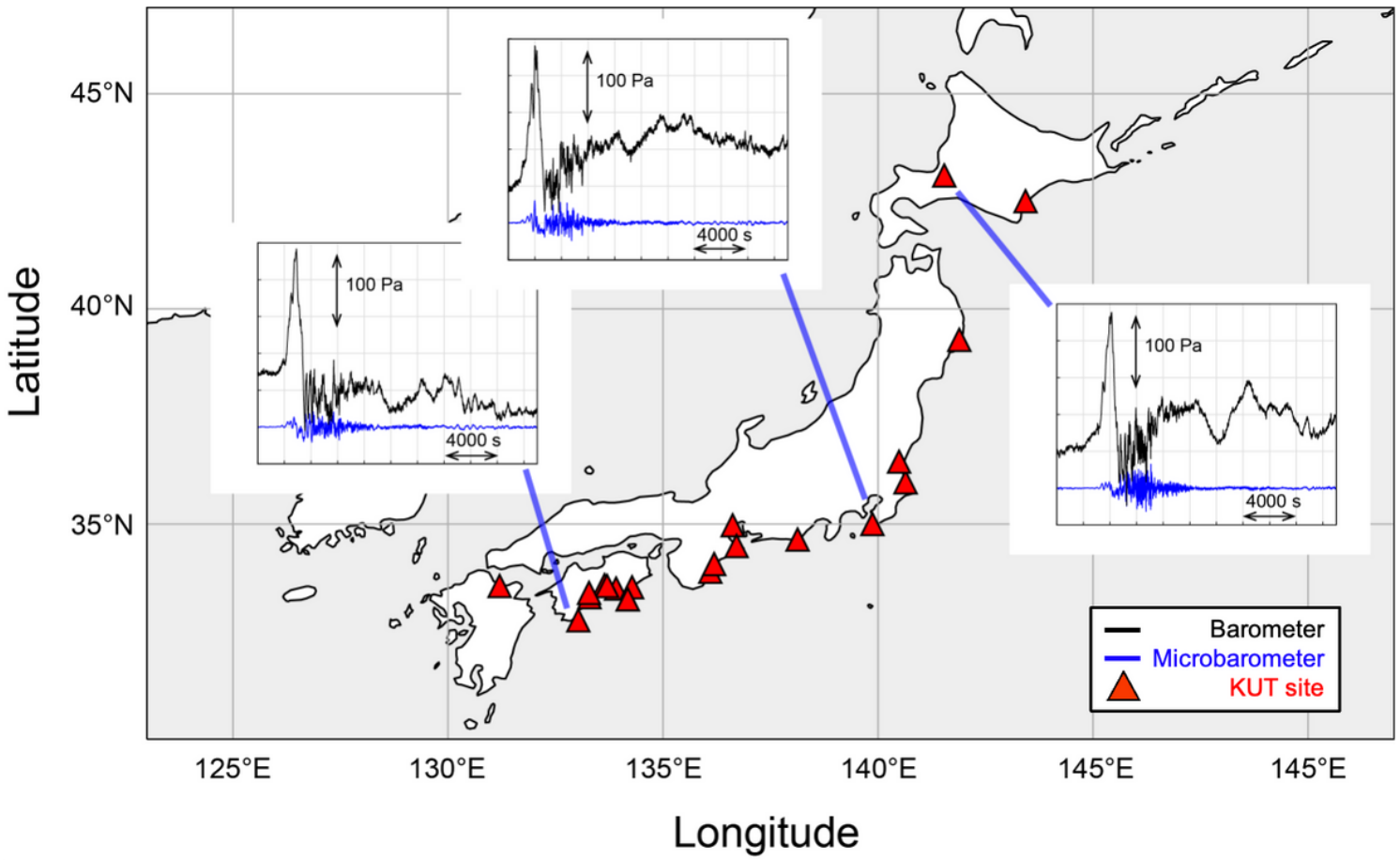

Figure 1

Location of Kochi University of Technology (KUT) infrasound sensors and their observed Tonga volcanic eruption atmospheric data. The KUT installed more than 30 infrasound sensors to form a Japan-wide infrasound observation network. Every site has a SAYA INF01-type comprehensive sensor that contains a membrane-type infrasound sensor, a barometer, a thermometer, and a three-component accelerometer of small MEMS sensor chips. These observation sites are 7,700 to 8,400 km away from Tonga, and the pressure fluctuations were monitored approximately 7 hours after the eruption. Examples of time series of pressure perturbation are shown; the observed signals had similar waveforms regardless of their locations.

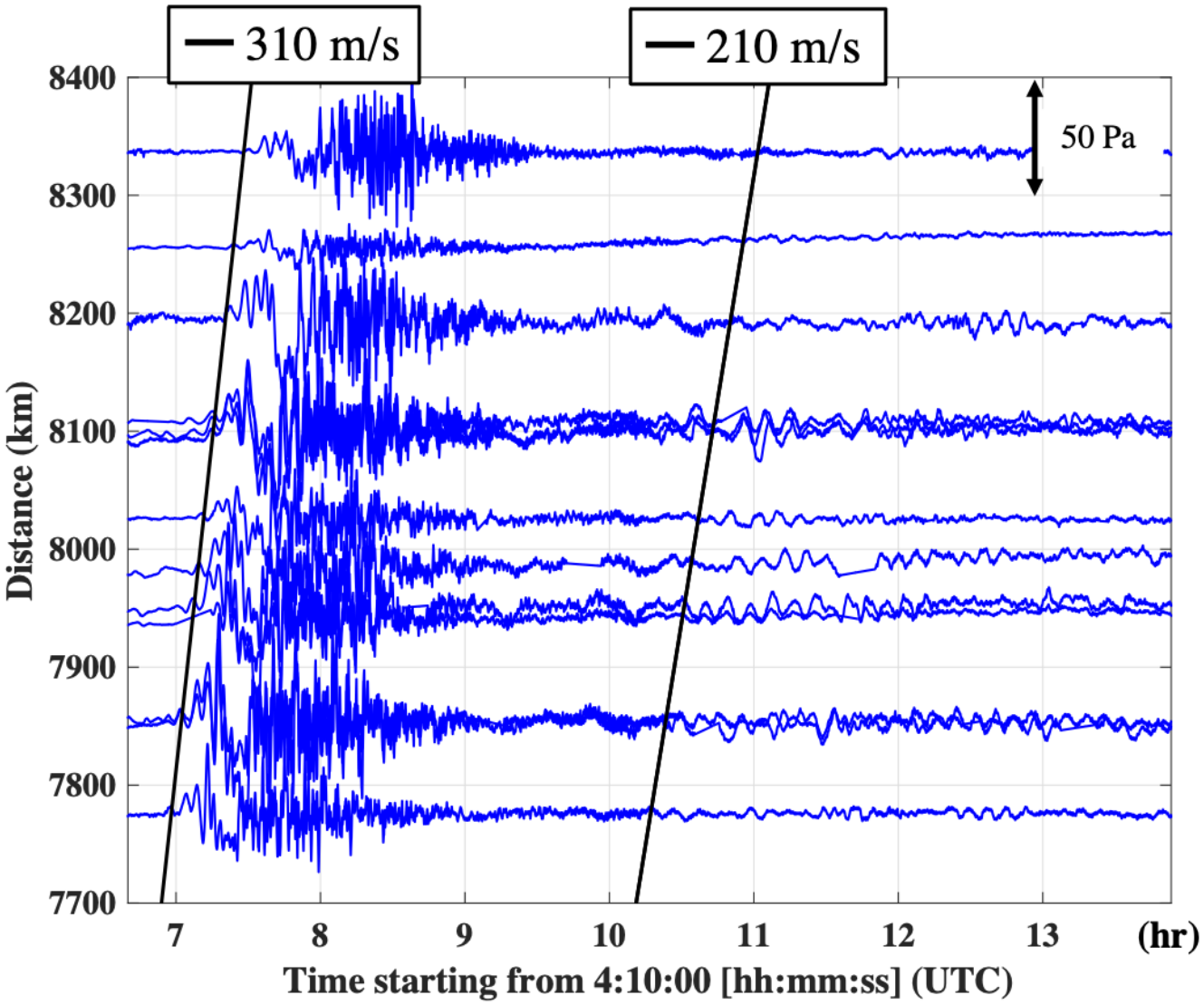

Figure 2

Waveforms obtained by the KUT infrasound network at 7,700–8,400 km from the Tonga volcano. The Lamb wave with 310 m/s celerity was observed 7 hours after the eruption; the shapes of the waveforms are similar for every location in Japan. Several hours after the Lamb wave, long-lasting gravity waves, 210 m/s wave celerity, were also observed all over Japan.

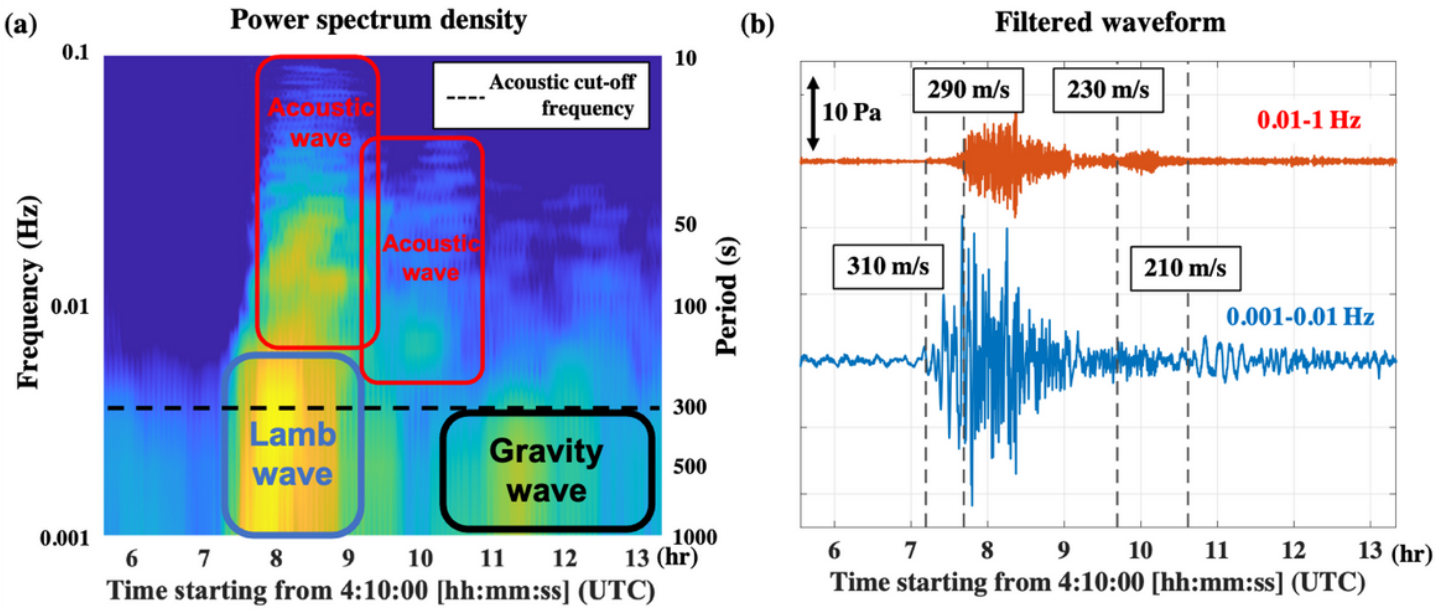

Figure 3

Time series of the atmospheric pressure perturbations at Muroto, Kochi (N33.25, E134.18). (a) Power spectrum density of atmospheric pressure waves and (b) filtered signals by two frequency ranges. Rectangles in (a) present each wave type's frequency and time range. The lower frequency Lamb wave arrives first (310 m/s), followed by the acoustic (290 and 230 m/s) and gravity waves of higher frequency. The last gravity wave, whose velocity matched a tsunami (200-220 m/s), caused Proudman resonance and excited the tsunami on the Pacific Ocean.

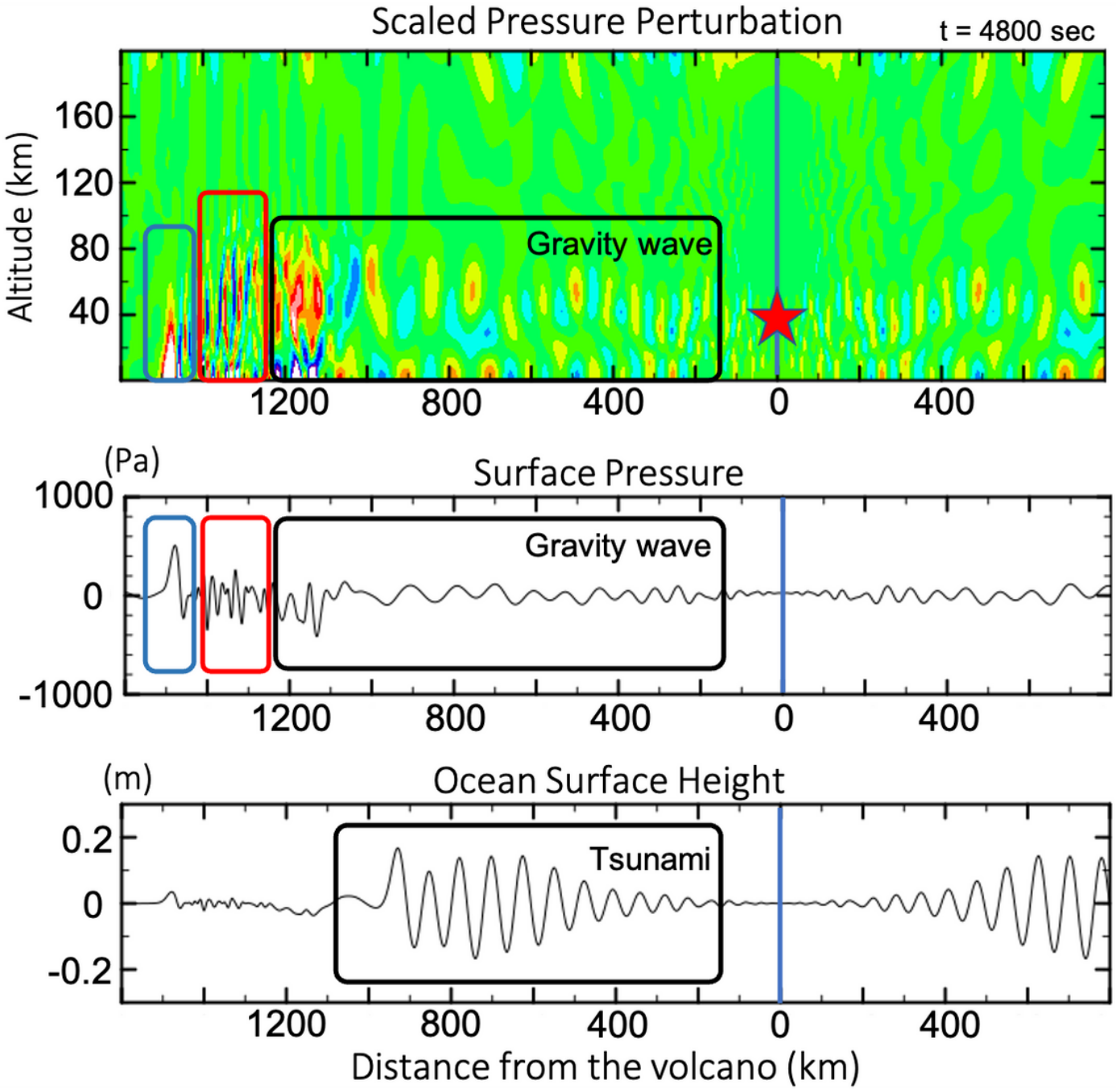

Figure 4

Pressure perturbations and ocean surface height simulated by a hydrodynamic model, including the coupling of atmosphere and tsunami. A localized heat source (indicated by the star) is initially given and excites various atmospheric waves. Lamb wave (blue rectangle) propagates, being trapped near the sea surface at the sound velocity. Acoustic waves (red rectangle) immediately follow, bouncing between mesopause (altitude of ~100 km) and the sea surface. Then, gravity waves (black rectangle) follow, being trapped below the mesopause. The gravity waves propagate with a variety of velocities depending on the horizontal wavelength and vertical structure, and some of them propagate with the phase velocity

of ~200 m/s that resonate with tsunamis for the ocean depths of 4000 m, resulting in large-amplitude tsunamis (See Supplementary movie for temporal evolution).

Supplementary Files

This is a list of supplementary files associated with this preprint. Click to download.

- MethodsNC.docx
- ExtendedDataNC.docx
- Sypplementarymovie.mpg